REPORT DOCUMENTATION PAGE

Form Approved OMB NO. 0704-0188

1. REPORT DATE (DD-MM-YYYY)	2. REPORT TYPE	3. DATES COVERED (From - To)
03-01-2012	Final Report	15-May-2008 - 30-Oct-2011

4. TITLE AND SUBTITLE
Programmable Matter - Final Report

5a. CONTRACT NUMBER
W911NF-08-1-0143

5b. GRANT NUMBER

5c. PROGRAM ELEMENT NUMBER
8D10AN

6. AUTHORS
George M. Whitesides, Michael Brenner, Zhigang Suo, L. Mahadevan, Ralph Nuzzo, Bartosz Grzybowski

5d. PROJECT NUMBER

5e. TASK NUMBER

5f. WORK UNIT NUMBER

7. PERFORMING ORGANIZATION NAMES AND ADDRESSES
Harvard University
Office of Sponsored Research
1350 Massachusetts Ave. Holyoke 727
Cambridge, MA 02138 -

8. PERFORMING ORGANIZATION REPORT NUMBER

9. SPONSORING/MONITORING AGENCY NAME(S) AND ADDRESS(ES)
U.S. Army Research Office
P.O. Box 12211
Research Triangle Park, NC 27709-2211

10. SPONSOR/MONITOR'S ACRONYM(S)
ARO

11. SPONSOR/MONITOR'S REPORT NUMBER(S)
54537-MS-DRP.9

12. DISTRIBUTION AVAILIBILITY STATEMENT
Approved for Public Release; Distribution Unlimited

13. SUPPLEMENTARY NOTES
The views, opinions and/or findings contained in this report are those of the author(s) and should not contrued as an official Department of the Army position, policy or decision, unless so designated by other documentation.

14. ABSTRACT
Our final report for this program summerizes how we (Harvard) have greatly improved our understanding of assembly using magnetic levitation, and mechanical agitation. Additionally, we report on how we have developed several types of soft-actuators that change compliance and shape based on pneumatic pressurization.
The Nuzzo group (University of Illinois, Urbana-Champaign) describe a new form of stimuli-responsive polymeric actuator—a chemically-driven, mechano-polymer—that provides a new approach to effecting efficient,

15. SUBJECT TERMS
programmable matter, magnetic self-assembly, magnetic fields, hydrogel actuator, nanoparticles, negatively charged particles

16. SECURITY CLASSIFICATION OF:			17. LIMITATION OF ABSTRACT	15. NUMBER OF PAGES	19a. NAME OF RESPONSIBLE PERSON
a. REPORT	b. ABSTRACT	c. THIS PAGE			George Whitesides
UU	UU	UU	UU		19b. TELEPHONE NUMBER: 617-495-9430

Report Title

Programmable Matter - Final Report

ABSTRACT

Our final report for this program summerizes how we (Harvard) have greatly improved our understanding of assembly using magnetic levitation, and mechanical agitation. Additionally, we report on how we have developed several types of soft-actuators that change compliance and shape based on pneumatic pressurization.
The Nuzzo group (University of Illinois, Urbana-Champaign) describe a new form of stimuli-responsive polymeric actuator—a chemically-driven, mechano-polymer—that provides a new approach to effecting efficient, multidimensional and potentially "smart" programmable movements.
The Grzybowski group (Northwestern) report on how they employ precisely controlled, to a micrometer scale, external magnetic fields to direct assembly of nonmagnetic and magnetic colloidal systems into colloidal crystals or core-shell assemblies.

Enter List of papers submitted or published that acknowledge ARO support from the start of the project to the date of this printing. List the papers, including journal references, in the following categories:

(a) Papers published in peer-reviewed journals (N/A for none)

Received	Paper
2012/01/03 1(8	Madhav Mani, George Whitesides, Michael Brenner, Filip Ilievski. Self-assembly of magnetically interacting cubes by a turbulent fluid flow, Physical Review E, (01 2011): 0. doi: 10.1103/PhysRevE.83.017301
2012/01/03 1(7	Filip Ilievski, Aaron D. Mazzeo, Robert F. Shepherd, Xin Chen, George M. Whitesides. Soft Robotics for Chemists, Angewandte Chemie International Edition, (02 2011): 0. doi: 10.1002/anie.201006464
2012/01/03 1(6	Sindy K.Y. Tang, Ratmir Derda, Aaron D. Mazzeo, George M. Whitesides. Reconfigurable Self-Assembly of Mesoscale Optical Components at a Liquid-Liquid Interface, Advanced Materials, (06 2011): 0. doi: 10.1002/adma.201100067
2012/01/03 1(5	Katherine A. Mirica, Filip Ilievski, Audrey K. Ellerbee, Sergey S. Shevkoplyas, George M. Whitesides. Using Magnetic Levitation for Three Dimensional Self-Assembly, Advanced Materials, (09 2011): 0. doi: 10.1002/adma.201101917

TOTAL: 4

Number of Papers published in peer-reviewed journals:

(b) Papers published in non-peer-reviewed journals (N/A for none)

Received	Paper

TOTAL:

Number of Papers published in non peer-reviewed journals:

(c) Presentations

Number of Presentations: 0.00

Non Peer-Reviewed Conference Proceeding publications (other than abstracts):

Received	Paper

TOTAL:

Number of Non Peer-Reviewed Conference Proceeding publications (other than abstracts):

Peer-Reviewed Conference Proceeding publications (other than abstracts):

Received	Paper

TOTAL:

Number of Peer-Reviewed Conference Proceeding publications (other than abstracts):

(d) Manuscripts

Received	Paper	
2012/01/19 15	3	Sindy K.Y. Tang, Ratmir Derda, Aaron D. Mazzeo, George M. Whitesides. Reconfigurable Self-Assembly of Mesoscale OpticalComponents at a Liquid–Liquid Interface, Advanced Materials ( )
2012/01/19 15	1	Filip Ilievski, Madhav Mani, George M. Whitesides, Michael P. Brenner. Self-Assembly of Magnetically Interacting Cubes by a Turbulent Fluid Flow, Physical Review E ( )
2012/01/19 15	4	George M. Whitesides, Katherine Mirica, Audrey Ellerbee, Sergey S. Shevkoplyas. Using Magnetic Levitation for Three Dimensional Self-Assembly, Advanced Materials ( )

TOTAL: **3**

Number of Manuscripts:

Books

Received	Paper

TOTAL:

Patents Submitted

Quality Control for Plastic Injection,
G.M. Whitesides, S Tricard, A.K. Ellerbee PCT/US/11/62399 filed 11/29/11

Soft Robotics for Chemists,
G.M. Whitesides, Z. Nie, R.F. Shepherd, F. Ilievski, X.Chen, R. Martinez, W.J. Choi, A.D. Mazzeo, S.Morin, S.W. Kwok, A.Stokes
PCT/US11/61720 filed 11/21/11

Method for Measuring "Closeness" in a Network
L. Mahadevan, G.C. Morrison
13/230,496 filed 9/12/11

On-Demand and Reversible Drug Release by External Cue
Z. Suo, D.J. Mooney, N.D. Huebsch, X, Zhao

Patents Awarded

Awards

None during reporting period

Graduate Students

NAME	PERCENT_SUPPORTED	Discipline
Gregory Morrison	0.25	
FTE Equivalent:	**0.25**	
Total Number:	**1**	

Names of Post Doctorates

NAME	PERCENT_SUPPORTED
Ramses Martinez	0.25
Robert Shepherd	0.25
Filip Ilievski	1.00
Adam Stokes	0.75
Manza Atkinson	0.50
Ahmet Faik Demirors	1.00
FTE Equivalent:	**3.75**
Total Number:	**6**

Names of Faculty Supported

NAME	PERCENT_SUPPORTED	National Academy Member
George M. Whitesides	0.01	Yes
Zhigang Suo	0.10	
Michael Brenner	0.10	No
L. Mahadevan	0.00	
Ralph Nuzzo	0.10	
Bartosz Grzybowski	0.10	
FTE Equivalent:	**0.41**	
Total Number:	**6**	

Names of Under Graduate students supported

NAME	PERCENT_SUPPORTED
FTE Equivalent:	
Total Number:	

Student Metrics

This section only applies to graduating undergraduates supported by this agreement in this reporting period

The number of undergraduates funded by this agreement who graduated during this period:	0.00
The number of undergraduates funded by this agreement who graduated during this period with a degree in science, mathematics, engineering, or technology fields:	0.00
The number of undergraduates funded by your agreement who graduated during this period and will continue to pursue a graduate or Ph.D. degree in science, mathematics, engineering, or technology fields:	0.00
Number of graduating undergraduates who achieved a 3.5 GPA to 4.0 (4.0 max scale):	0.00
Number of graduating undergraduates funded by a DoD funded Center of Excellence grant for Education, Research and Engineering:	0.00
The number of undergraduates funded by your agreement who graduated during this period and intend to work for the Department of Defense	0.00
The number of undergraduates funded by your agreement who graduated during this period and will receive scholarships or fellowships for further studies in science, mathematics, engineering or technology fields:	0.00

Names of Personnel receiving masters degrees

NAME
Total Number:

Names of personnel receiving PHDs

NAME
Total Number:

Names of other research staff

NAME	PERCENT_SUPPORTED
T.J. Martin	0.40
Tracie Smart	0.15
FTE Equivalent:	**0.55**
Total Number:	**2**

Sub Contractors (DD882)

1 a. Northwestern University Evanston Campus

1 b. Office for Sponsored Research
Northwestern University
Evanston IL 602081110

Sub Contractor Numbers (c):
Patent Clause Number (d-1):
Patent Date (d-2):
Work Description (e): The Grzybowski lab specializes in experimental and theoretically complex systems. Their work will
Sub Contract Award Date (f-1): 5/15/2008 12:00:00AM
Sub Contract Est Completion Date(f-2): 10/30/2011 12:00:00AM

---

1 a. Northwestern University Evanston Campus

1 b. Research and Sponsored Programs
633 Clark Street
Evanston IL 602081110

Sub Contractor Numbers (c):
Patent Clause Number (d-1):
Patent Date (d-2):
Work Description (e): The Grzybowski lab specializes in experimental and theoretically complex systems. Their work will
Sub Contract Award Date (f-1): 5/15/2008 12:00:00AM
Sub Contract Est Completion Date(f-2): 10/30/2011 12:00:00AM

---

1 a. University of Illinois - Urbana - Champaign

1 b. Office of Sponsored Programs
1901 S. First Street
Champaign IL 61820

Sub Contractor Numbers (c):
Patent Clause Number (d-1):
Patent Date (d-2):
Work Description (e): The Nuzzo lab specializes in desigining, developing, and analyzing systems of components. Their r
Sub Contract Award Date (f-1): 5/15/2008 12:00:00AM
Sub Contract Est Completion Date(f-2): 10/30/2011 12:00:00AM

---

1 a. University of Illinois - Urbana - Champaign

1 b. Grants & Contracts Office
Office of Business & Financial Services
Champaign IL 618207406

Sub Contractor Numbers (c):
Patent Clause Number (d-1):
Patent Date (d-2):
Work Description (e): The Nuzzo lab specializes in desigining, developing, and analyzing systems of components. Their r
Sub Contract Award Date (f-1): 5/15/2008 12:00:00AM
Sub Contract Est Completion Date(f-2): 10/30/2011 12:00:00AM

Inventions (DD882)

5 **MagLev Self Assembly**

Patent Filed in US? (5d-1) Y

Patent Filed in Foreign Countries? (5d-2) N

Was the assignment forwarded to the contracting officer? (5e) N

Foreign Countries of application (5g-2):

5a: George M. Whitesides

5f-1a: President and Fellows of Harvard College

5f-c: 1350 Massachusetts Ave

Cambridge MA 02138

5a: Sergey S. Shevkoplyas

5f-1a: President and Fellows of Harvard College

5f-c: 12 Oxford Street

Cambridge MA 02138

5a: Audrey Ellerbee

5f-1a: President and Fellows of Harvard College

5f-c: 12 Oxford Street

Cambridge MA 02138

5a: Filip Ilievski

5f-1a: President and Fellows of Harvard College

5f-c: 12 Oxford Street

Cambridge MA 02138

5 **Method for Measuring "Closness" in a network**

Patent Filed in US? (5d-1) Y

Patent Filed in Foreign Countries? (5d-2) N

Was the assignment forwarded to the contracting officer? (5e) Y

Foreign Countries of application (5g-2):

5a: Gregory Charles Morrison

5f-1a: President and Fellows of Harvard College

5f-c: 29 Oxford Street

Cambridge MA 02138

5a: Lakshminarayanan Mahadevan

5f-1a: President and Fellows of Harvard College

5f-c: 1350 Massachusetts Avenue

Cambridge MA 02138

5 **On-demand and Reversible Drug Release by External Cue**

Patent Filed in US? (5d-1) Y

Patent Filed in Foreign Countries? (5d-2) Y

Was the assignment forwarded to the contracting officer? (5e) Y

Foreign Countries of application (5g-2): China, India, Japan, European Union

5a: Zhigang Suo

5f-1a: President and Fellows of Harvard College

5f-c: 1350 Massachusetts Avenue

Cambridge MA 02138

5a: David J Mooney

5f-1a: President and Fellows of Harvard College

5f-c: 29 Oxford Street

Cambridge MA 02138

5a: Nathaniel D. Huebsch

5f-1a: President and Fellows of Harvard College

5f-c: 29 Oxford Street

Cambridge MA 02138

5a: Xuanhe Zhao

5f-1a: President and Fellows of Harvard College

5f-c: 29 Oxford Street

Cambridge MA 02138

5 **Quality Control for Plastic Injection**

Patent Filed in US? (5d-1) Y

Patent Filed in Foreign Countries? (5d-2) N

Was the assignment forwarded to the contracting officer? (5e) N

Foreign Countries of application (5g-2):

5a: Audrey Ellerbee

5f-1a: President and Fellows of Harvard College

5f-c: 12 Oxford Street

Cambridge MA 02138

5a: George M. Whitesides

5f-1a: President and Fellows of Harvard College

5f-c: 1350 Massachusetts Ave

Cambridge MA 02138

5a: Simon Tricard

5f-1a: President and Fellows of Haravrd College

5f-c: 12 Oxford Street

Cambridge MA 02138

5 **Self assembly of magnetically interacting cubes by turbulent fluid flow**

Patent Filed in US? (5d-1) N

Patent Filed in Foreign Countries? (5d-2) N

Was the assignment forwarded to the contracting officer? (5e) N

Foreign Countries of application (5g-2):

5a: George M. Whitesides

5f-1a: President and Fellows of Harvard College

5f-c: 1350 Massachusetts Ave

Cambridge MA 02138

5 **Soft Robotics for Chemists**

Patent Filed in US? (5d-1) Y

Patent Filed in Foreign Countries? (5d-2) N

Was the assignment forwarded to the contracting officer? (5e) Y

Foreign Countries of application (5g-2):

5a: Won Jae Choi

5f-1a: President and Fellows of Harvard College

5f-c: 12 Oxford Street

Cambridge MA 02138

5a: Aaron Mazzeo

5f-1a: President and Fellows of Harvard College

5f-c: 12 Oxford Street

Cambridge MA 02138

5a: Stephen Morin

5f-1a: President and Fellows of Harvard College

5f-c: 12 Oxford Street

Cambridge MA 02138

5a: Sen Wai Kwok

5f-1a: President and Fellows of Harvard College

5f-c: 12 Oxford Street

Cambridge MA 02138

5a: Xin Chen

5f-1a: President and Fellows of Harvard College

5f-c: 12 Oxford Street

Cambridge MA 02138

5a: Filip Ilievski

5f-1a: President and Fellows of Harvard College

5f-c: 12 Oxford Street

Cambridge MA 02138

5a: Robert Foster Shepherd

5f-1a: President and Fellows of Harvard College

5f-c: 12 Oxford Street

Cambridge MA 02138

5a: Zhihong Nie

5f-1a: President and Fellows of Harvard College

5f-c: 12 Oxford Street

Cambridge MA 02138

5a: George M. Whitesides

5f-1a: President and Fellows of Harvard College

5f-c: 1350 Massachusetts Avenue

Cambridge MA 02138

5a: Ramses Martinez

5f-1a: President and Fellows of Harvard College

5f-c: 12 Oxford Street

Cambridge MA 02138

5a: Adam Stokes

5f-1a: President and Fellows of Harvard College

5f-c: 12 Oxford Street

Cambridge MA 02138

Scientific Progress

Please see attached.

Technology Transfer


PROGRAMMABLE MATTER

W911NF-08-1-0143

FINAL REPORT
8/1/11 – 10/31/11

DARPA/DSO
ATTN: BAA 10-65
Dr. Gill Pratt
3701 North Fairfax Drive
Arlington VA 22203-1714

Technical POC: Dr. Gill Pratt, DARPA/DSO
Submission: Gill.pratt@darpa.mil

Submission from:

George M. Whitesides
Department of Chemistry and Chemical Biology
Harvard University
Cambridge, MA 02138
gwhitesides@gmwgroup.harvard.edu
Tel: 617 495 9430
Fax: 617 495 9857

Laboratory Manager
T.J. Martin
tjmartin@gmwgroup.harvard.edu
Tel: 617 495 9432
Fax: 617 495 9857

OUTLINE

1. HARVARD UNIVERSITY (WHITESIDES GROUP)

This program has greatly improved our understanding of assembly using magnetic levitation, and mechanical agitation. Additionally, we have developed several types of soft-actuators that change compliance and shape based on pneumatic pressurization. From our new understanding, we have published four papers (1-4), and filed two patents. In this final report, we summarize our key findings.

1.1. PROGRAMMING THE SHAPE OF SELF-ASSEMBLED OBJECTS VIA MAGNETIC FIELDS

1.1.1. Introduction

In our prior Programmable Matter reports, we described the levitation and three-dimensional (3D) self-assembly (SA) of mm-sized diamagnetic objects, suspended in a paramagnetic liquid, in a non-uniform magnetic field. The method employed a device that consists of two permanent magnets oriented with like poles facing each other (anti-Helmholtz configuration), and a container filled with paramagnetic medium. We assembled objects in 3D by suspending them in paramagnetic medium, and positioning the container between the two magnets. The final positioning of these objects in the liquid and their self-assembly is directed by gravitational forces, magnetic forces, and steric interactions (physical contact) among and between the objects and the container.

In order to program the shape of the assembled objects, we adjust the shape of the magnetic field in which the levitation is performed, the average density of the levitating objects, as well as the density distribution of each component. By controlling these parameters, we have assembled discrete objects into hierarchical structures and then changed the shapes of the structures in-situ.

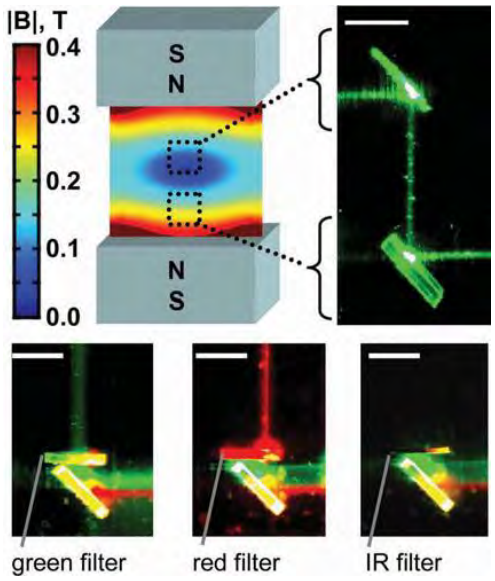

Fig. 1.1.2 (top, left) Magnetic field shape to align (top, right) two mirrors that guide a laser through (bottom, left-right) a green filter, red filter, and IR filter.(4)

1.1.2. Field mediated self-assembly

By applying permanent magnets of equal strength, in an anti-Helmholtz configuration, a gradient is established, with the largest field at the magnetic poles and the lowest field at the centre of the poles. Depending on the magnetic susceptibility of an object, it will position its centre of mass at different positions within this field gradient, w.r.t. the paramagnetic fluid in which it is suspended.

We have demonstrated the utility of this phenomenon by magnetically levitating mirrors and optical filters and then allowing them to self assemble. The result is a simple device that selectively filters an incident laser beam (Fig. 1.1.2) (4). We also demonstrated the utility of magnetic levitation to self assemble soft and hard millimetre scale components.

1.1.3. Field and template mediated self-assembly

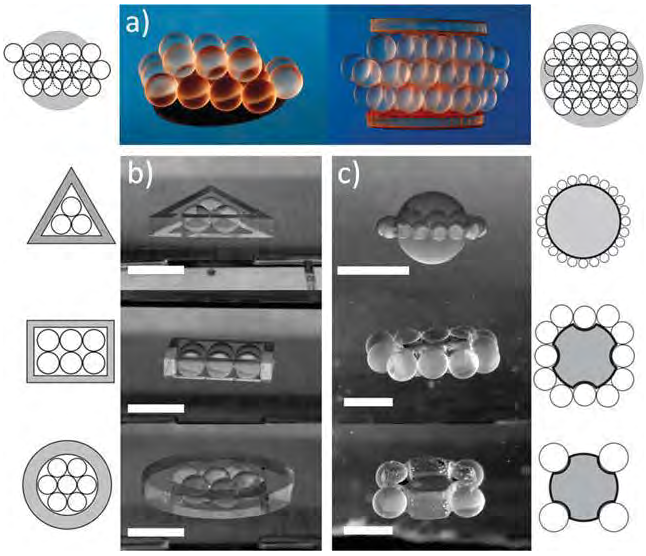

Figure 1.1.3 (top, left) Magnetic field shape to align (top, right) two mirrors that guide a laser through (bottom, left-right) a green filter, red filter, and IR filter.

Using only the magnetic field gradient for self-assembly does have some limitations – particularly, it does not currently provide a route for organization within a plane of equal field strength. To circumvent this limitation, we have incorporated levitating templates to direct the assembly of the levitating components within the field gradient (3). Fig. 1.1.3, a demonstrates templated assembly of magnetically levitated beads into an FCC packing.

In addition to templating assembly from the bottom up, we also directed the assembly internally to a template (Fig. 1.1.3, b) and externally from a template (Fig. 1.1.3, c).

1.2. SELF ASSEMBLY USING MECHANICAL AGITATION

1.2.1. Introduction

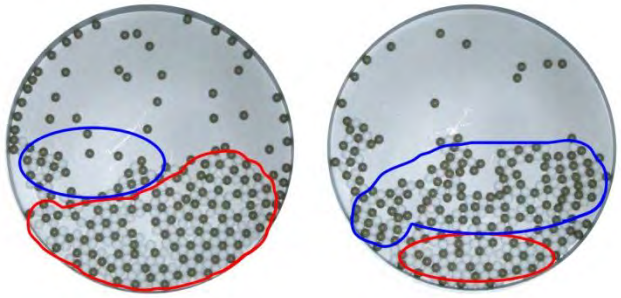

Figure 1.2.2 Photographs of Delrin (white) and Torlon (dark) spheres on an aluminum dish after agitation at for 90 sec and 150 seconds respectively. The lattice structure changed from predominately hexagonal (red) to predominately square (blue).

We continued to develop systems in which self-assembly is driven by electrostatic forces between particles that acquire electrical charge triboelectrically. The particles that we used in these studies were polymer spheres and cylinders which either charged positively, negatively, or remained neutral when shaken together inside containers with flat horizontal bottoms. We also started the development of systems that self-assemble without attractive directional interactions.

1.2.2.Energy dependent assembly

We studied the behavior of beads under different agitation conditions this led to the formation of various lattices depending on the rates of charging. When one type of bead charged quicker than the other the first structure formed was predominantly hexagonal. This structure could change to square when the number of both types of beads was equal and the energy was high enough to allow phase transition.

1.2.3.Finite size effects

We studied the influence of the dish size on the lattice formation of beads with a constant size. We found the structure was open with four to five beads of one type surrounding the beads of the other type when the size of the beads was large (d_{bead}~ 0.1 d_{dish}) compared to the size of the dish. When the size of the beads was small (d_{bead}~0.0003 d_{dish}) compared to the size of the dish, hexagonal structures formed. Towards the rim of the dish the hexagonal structures adopted more open conformations to follow the curvature of the dish.

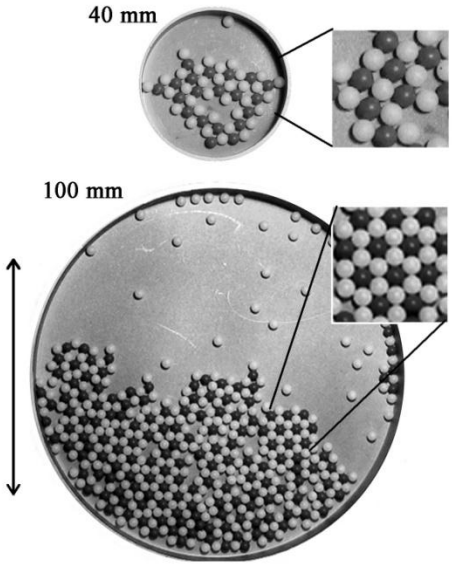

Figure 1.2.3 Photographs of Delrin (white) and Torlon (dark) spheres (d=3.18mm) in a 2:1 ratio on 40mm and 100mm aluminum dishes. In the large dish, beads formed close packed hexagonal crystals and some unordered areas. In the small dish, beads do not pack closely

1.2.4. Assembly in mixed systems

We studied the assembly of objects with different shapes, e.g. cubes and beads. The combination of these two objects in a 1:1 number ratio led to the formation of square structures independent of the shape of the objects; the main difference being that we needed higher agitation energies for cubes than for beads due to their inability to roll. When we changed the number ratio to 2:1 we formed unordered hexagonal structures if beads were in excess and square structures when cubes were in excess.

1.3. SOFT ACTUATORS AND ROBOTIC GRIPPER

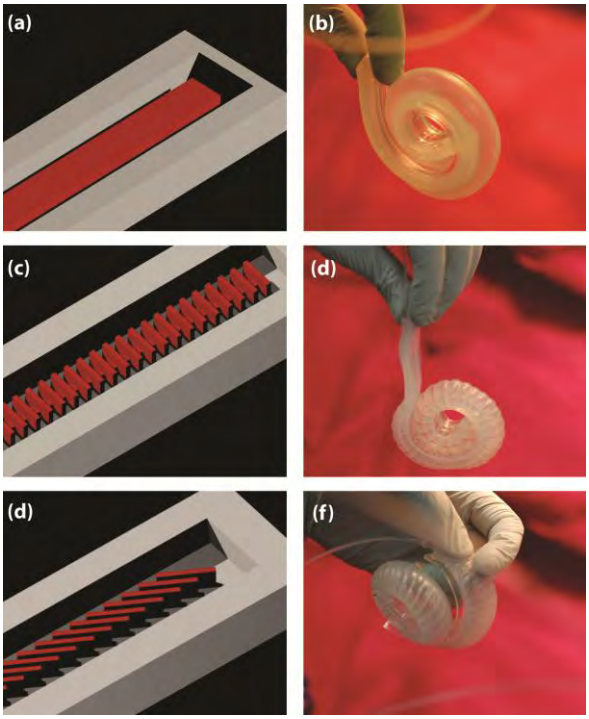

Figure 1.3.2 (a) mould used to replicate the actuator in (b). (c) mould with 90° channels(2)

1.3.1. Introduction

The shape and compliance of moulded elastomer networks can change upon pneumatic pressurization. We have developed two classes of soft actuators, based on pneumatically actuated elastomeric networks. We have then used one of these classes to assemble a soft robotic gripper (2).

1.3.2.Bending Actuator

When a typical balloon inflates, it does so isotropically. By fixing one side of the balloon, and inflating, it will curl around the fixed side. In this program, we used soft lithography to fabricate inflatable channels in ultrasoft elastomers (pneu-nets) and then we programmed their inflation to cause bending (Fig. 1.3.2a, b). Previously, soft lithography relied on replicating silicone from moulds patterned using photo-lithography; these moulds are usually simple 2D extrusions. In this program, we used a 3D printer to fabricate moulds with topography – a new development in soft lithography. By varying the position and angle of the channels on the mould, we were able to change the mode of bending of the replicated pneu-net from in plane (Fig. 1.3c, d) to a helical out of plane bending (Fig. 1.3d, e).

1.3.3.Reverse Curl

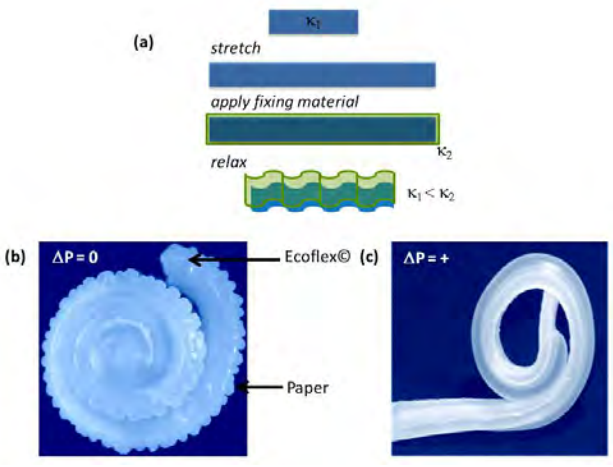

Figure 1.3.3. (a) Low stiffness material is stretched and then high stiffness material is chemically bonded to the surface of the stretched material. Upon relaxation of the strain, the low stiffness material attempts to return to its original dimensions by buckling the high stiffness material. (b) The rest state of the strain patterned composite is a coiled strip that (c) extends upon pressurization.

We have also fabricated an *extending actuator* which begins in a coiled state and extends/straightens upon pressurization. We used our 3D printing device to form a negative mould of a pneumatic channel and mould this channel using low stiffness Ecoflex ©. This soft channel is then uniaxially strained and the

strain state is permanently patterned into the pneumatic channel by bonding a high stiffness material, such as paper, to one side of the channel, Figure a. Figure b is the result of this patterning using Ecoflex© as the channel material and paper as the strain fixing material, clearly the paper buckles as the channel relaxes some of the initial strain. Figure c is the result of pressurizing the channel in Figure b. As the microchannel stretches to reach the degree of strain encountered when the paper was affixed, the buckling disappears and the microchannel extends. Possible uses of this soft actuation mode are chameleon tongue like grabbers, frog-like jumpers, and unfurling of sheets like sails.

1.3.4.Gripper

We arranged the bending actuators from section 1.3.2 into a gripping device (Fig. 1.3.4). Essentially, six pneu-nets, similar to those in Fig. 1.3.2c, d, where arranged at 60^{o} to one-another in a planar array. We connected all six pneu-nets to a single pressure source–when we applied pressure, the gripper curled around an object. (2)

The compliant nature of the gripper allows it to wrap around irregularly shaped objects; additionally, the low pressures required to actuate the gripper allows it to handle delicate objects: We used this gripper to pick up an uncooked chicken egg and a live mouse without damaging them and without complex sensory feedback.

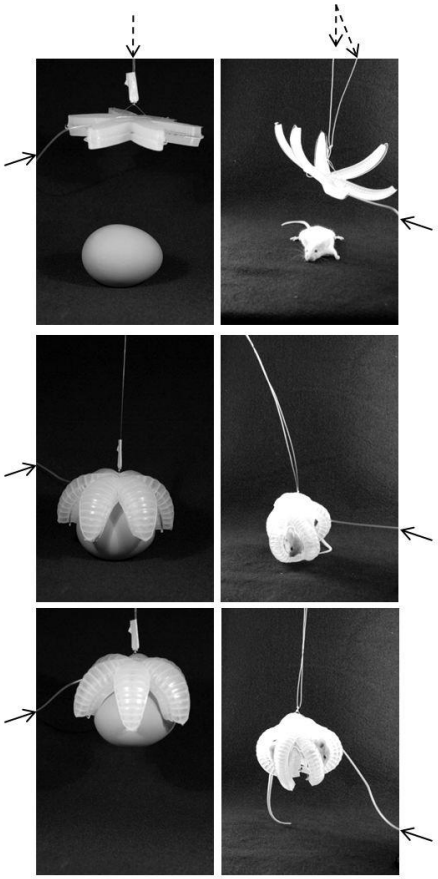

Figure 1.3.4. (left, top to bottom) A gripper picks up an uncooked chicken egg without breaking it. (right, top to bottom) A larger gripper picks up a live, anesthetized mouse without hurting it.

1.3.5. Reverse Gripper

Using a similar concept to the gripper based on bending actuation, we arranged the reverse curling actuators from section 1.3.3 to create a "reverse" gripper. This gripper uses pressure to actuate, but maintains grip in the rest state – without the need to continue applying pressure (Fig. 1.3.5).

We have used this gripper to pick up a variety of irregular objects (Fig. 1.3.5, e-g).

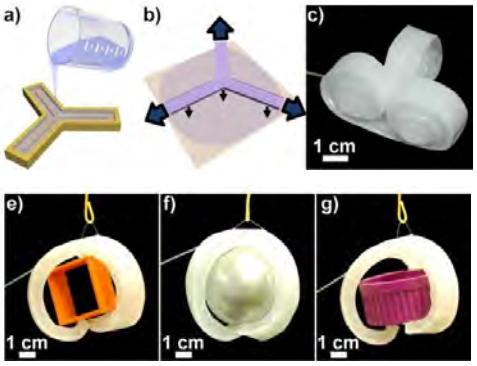

Figure 1.3.5. Process to fabricate a reverse gripper by bonding a prestretched Ecoflex body against paper. (e-g) Gripping different shapes: a frame, an sphere and a plastic cup.

REFERENCES

1 Ilievski F, Mani M, Whitesides GM, & Brenner MP (2011) Self-assembly of magnetically interacting cubes by a turbulent fluid flow. *Physical Review E* 83(1).

2. Ilievski F, Mazzeo AD, Shepherd RE, Chen X, & Whitesides GM (2011) Soft Robotics for Chemists. *Angewandte Chemie-International Edition* 50(8):1890-1895.

3. Ilievski F, Mirica KA, Ellerbee AK, & Whitesides GM (2011) Templated self-assembly in three dimensions using magnetic levitation. *Soft Matter* 7(19):9113-9118.

4. Mirica KA, Ilievski F, Ellerbee AK, Shevkoplyas SS, & Whitesides GM (2011) Using Magnetic Levitation for Three Dimensional Self-Assembly. *Advanced Materials* 23(36):4134.

2. UNIVERSITY OF ILLINOIS, URBANA-CHAMPAIGN (NUZZO GROUP)

2.1. DRIVEN, LIGHT PROGRAMMABLE HYDROGEL ACTUATOR

We describe a new form of stimuli-responsive polymeric actuator—a chemically-driven, mechano-polymer—that provides a new approach to effecting efficient, multidimensional and potentially "smart" programmable movements. Prior work has provided numerous methods to trigger mechanical responses in organic actuators including, as examples: pH[1]; electric field[2]; ion concentration[3]; and chemical or biological reagents[4,5]. Among the varying types of external stimuli that have been explored, light driven mechanics have provided one of the most efficient and direct methods to achieve a programmable form of mechanical actuation[6.] This study focuses on eliciting a different form of light triggered mechano-chemical actuation, one that elicits photochemically programmed mechanical responses that in turn might be harnessed to drive hierarchical forms of assembly/motion that are in fact dissipatively driven.

In this model system (one demonstrating a proof of principles for this class of phase change material), we use visible light (ν ca. 450 nm) to trigger a peroxide coupled water splitting reaction that produces protons, which subsequently induce movements in pH responsive hydrogels. A schematic illustration of the light induced hydrogel response system is shown in Fig. 1a. Ruthenium (II)-trisbipyridine complexes have been shown to be an effective photosensitizing agent for this coupled sequence of reactions[7,8]. The photostimulated conversion of persulfate at pH ~5 is particularly effective. This value is also appropriate for constructing an acid-modifiable pH sensitive hydrogel. For this demonstration we choose a polymer gel based on a polyacrylic acid backbone, because it affords transition pH value of exactly 5, thus matching the activity profile of the ruthenium trisbipyridine complex. In the secondary couple, metal oxide nanoparticles are used as the functional catalyst in the water-splitting reaction. We used in this case IrO2 for reasons of its well-known, and highly efficient, catalytic activity and stability under oxidizing conditions[9,10.]

The chemistry used to construct the gel is a standard photo initiated polymerization under irradiation at 365 UV light. Acrylic acid (monomer, 175 mg, 2.4mM), methacrylate modified Ru(II)-tribipyridine (photosensitizer monomer, 1mg, $1.5x10^{-3}$mM) and N,N-methylenebis acrylamide (crosslinker, 5.00 mg, 0.03 mM) were dissolved in 1mL dimethyl sulfoxide (DMSO):H_2O=1:1 (v/v) , then adding in DAROCUR 1173 (photoinitiator, 30 μL,$1.8x10^{-4}$ mM) to form the pre-gel solution. This chemistry allows facile prototyping of actuating objects using projection masks to shape the optic field. The gel is immersed in an IrO2 nanoparticle suspension overnight before application. This treatment strongly (essentially irreversibly) entrains the oxide nanoparticles in the gel, presumably via an associative binding to the positively charged Ru(II) segments in the polymer network (the IrO2 nanoparticles are stabilized against aggregation by coordination to negatively charged citrate groups during its synthesis).[11] In a prototypical demonstration, the composite gel is immersed in an air saturated water solution that has a pH value

equaling 5.6(Fig. 1b-1), since the concentration of CO2 is about $3.5x10^{-4}$ atm. Under light exposure in the presence of the reagent $Na_2S_2O_8$ ($3.3x10^{-4}$M), a catalytic water splitting reaction is initiated that oxidizes H_2O, liberating oxygen and a correlated flux of protons. It is the latter elicit a subsequent localized decrease in pH. The latter change in pH value induces a swelling in the pH sensitive hydrogel (Fig. 1b-2)[12,13]. Terminating the irradiation shuts down the water splitting reaction. The pH of the solution begins to recover, as a result—by consuming HCO_3^- in the system bath, the protons produced through water-splitting reaction can be partially neutralized. As the pH value increases again, the dimensions of the pH sensitive gel are partially restored (Fig. 1b-3). These are behaviors that operate in what is essentially a weak buffer limit.

These mechanics were harnessed to demonstrate an improved design—a double-layered hydrogel actuator, which can effect several cycles of reversible shape changes, ones that are self-sustained by contact with the ambient environment and fully controllable in phase by light. In the last report, we suggested a prototype of a promising integration strategy for an actuator, by combining 2 layers of hydrogels as a bimorph: (a) Ru(II) trisbipyridine monomer segment incorporated poly acrylic acid (Ru-PAA), which has the same formula as described above; (b) poly-hydroxyethyl methacrylate (PHEMA), which is photopolymerized from a mixture of deionized water (solvent, 1.5 g, 83 mmol), 2-hydroxyethyl methacrylate (monomer, 3.0 g, 23 mmol), ethylene glycoldimethacrylate (crosslinker, 60 mg, 0.3 mmol) (1.1 wt.%), and 2,2-dimethoxy-2-phenyl-acetophenone (photoinitiator, 195.0 mg, 0.76 mmol)[14]. In the new design the two pre-gel phases are set side by side and photopolymerized in a single layer gel, as shown in Fig. 2a. The pre-gel solutions as currently formulated scatter the incidented light so irradiance levels through the gel are not even. This feature embeds an intrinsic strain in the polymerized bimorph, generating a spontaneous curvature due to the gradient change in crosslinking density vertically, which is further discontinuous at the material boundary in the curved structure. The light driven water splitting reaction leads the Ru-PAA end to deswell, which reduces the swelling ratio differences between the top and bottom regions of the gel, thus relaxing its curvature. The PHEMA domain has no phase change capacity for this reason does not undergo any obvious change in volume. It is however moved in translation by the dynamics of the Ru-PAA gel (Fig. 2b). After the system was moved to the dark state, the gel begins to recover (Fig. 2c). The resulting asymmetric swell and deswell in between two ends of a single layer gel creates a walking motion, as shown in the plot (Fig. 2d) of tracking the position of the gel.

As currently formulated, the light programmable system does not fully recover the initial (pre-light) pH state (and thus bimorph strain), requiring as a result changing the solution environment to restore the initial curvature. Even though the protons can be continuously produced stably in this pH range, the consumption of the protons is solely dependent upon the following reaction (absent other reagents):

$$H_2CO_3 \leftrightarrow H^+ + HCO_3^- \qquad \text{pKa=6.35} \qquad \text{(eq.1)}$$

The amount of bicarbonate is fixed by the concentration of initially CO_2 saturated solution. Given that the initial pH value equals 5.5, the new pH value reached at equilibrium post irradiance is 5.16. To fully optimize the actuator in a multi-cycle context will require an addition of a specific buffering system that does not impede the formation of the local pH gradient needed to drive the gel phase change response yet still effectively recovers an initial (more basic) swollen state in the PAA gel segments. Solid carbonates and other proton neutralizing additives are currently being examined to this end.

2.2. STRETCHABLE ELECTRODES EMBEDDED WITH A PH-RESPONSIVE POLYMERIC ACTUATOR

Previous work[15] has demonstrated that, by performing the oxygen reduction reaction (ORR) in a microfluidic ambient, the electrochemical process can produce remarkable pH gradients in between working electrode (WE) and counter electrode (CE). The magnitude of these gradients is sufficient to induce a gradient change in the volume of essentially any pH responsive gel. We have developed a new system that allows us to exploit such gradients in a new form of polymeric actuator, one embedding stretchable electrodes of a microelectrochemical reactor into the pH responsive polymer network.

The fabrication of programmable hydrogel devices mainly includes fabricating stretchable electronic meshes on a Si or glass substrate, followed by transferring them onto a carrier substrate, and finally embedded the array into a responsive hydrogel matrix through photo patterning. The fabrication starts from depositing a sacrificial layer of PMMA on Si substrate in order to provide a means to release the electrode mesh. A thin polyimide layer is then deposited, followed by the steps to construct the active electrical components, in this case the pH actuating electrodes. Another polyimide layer is then deposited to sandwich the electrical components (Fig. 3a). The meshes are then completed by dry etching in an oxygen plasma. The sacrificial PMMA layer is then stripped in acetone, and the electrode meshes transferred onto a carrier substrate through several steps of transfer printing using a PDMS stamp and thermal release tape (Fig. 3b). After connecting with a cable for wiring out the bus connections, the electronic meshes, after being transferred onto a glass substrate (Fig. 3c), are incorporated within the hydrogel. To do so, a prepared monomer solution is poured into a container where the electronic meshes are then floated over it (Fig. 3d). The hydrogel prepolymer is then photopolymerized using a mask to align the electrical array with the polymer shape's design. In order to sandwich the electronic mesh into the receiving hydrogel, a second hydrogel prepolymer solution is then added and polymerized in registry through the same mask. The polymerized hydrogel with embedded array is then immersed into water to remove residual monomers, solvents, and initiator.

Similar to the previous bimorph design, we used photolithography to pattern the gel with a gradient crosslink motif. The top layer in this case is poly acrylamide (PAAm) and the bottom layer poly acrylic acid (PAA). In 1mL of reactants, the pre-gel solution of PAAm contains acrylamide (monomer, 175 mg, 2.4mM), N,N'-methylenebis acrylamide(crosslinker, 20 mg, 0.1 mM) and Darocur 1173(photoinitiator, 30

μL,1.8x10^{-4} mM). The PAA layer of the bimorph incorporates acrylic acid (monomer, 175 mg, 2.4mM), N, N'-methylenebis acrylamide (crosslinker, 20 mg, 0.03mM), methacryloxyethyl thiocarbamoyl rhodamine B (photo curable dye, 1mg, 1.5x10^{-3}mM), and Darocur 1173 (photoinitiator, 30 μL, 1.8x10^{-4} mM) in 1 mL pre-gel solution. We used a lesser amount of crosslinkerer in this PAA gel is to maximize the swelling difference of the two layers, The pink colored rhodamine dye in PAA serves to differentiate the two layers (Fig. 3e).

The electrodes, once integrated in the bimorph gel, are immersed at a 0.1M KCl solution with pH=4, in order to achieve maximum strain change (the pKa of acrylic acid is 4.35). The electrochemical ORR is performed by applying a -1.1 V potential to the WE vs. a Ag pseudo reference. As the ORR proceeds, the WE performs the reaction:

$$O_2 + 4H^+ + 4e^- = 2H_2O \qquad \text{(eq.2)}$$

This partial reaction locally increases the pH value in the vicinity of the WE by consuming protons, leading the PAA layer to swell and induce curvature (Fig. 3f). We are working at these early stages of this project to enhance both the magnitude and reversibility of the pH responsiveness of the hydrogel strain mediated through the ORR. We believe this type of hybrid design—one embedding an active device level—provides the most explicit means for constructing efficient phase change based actuators.

Figures:

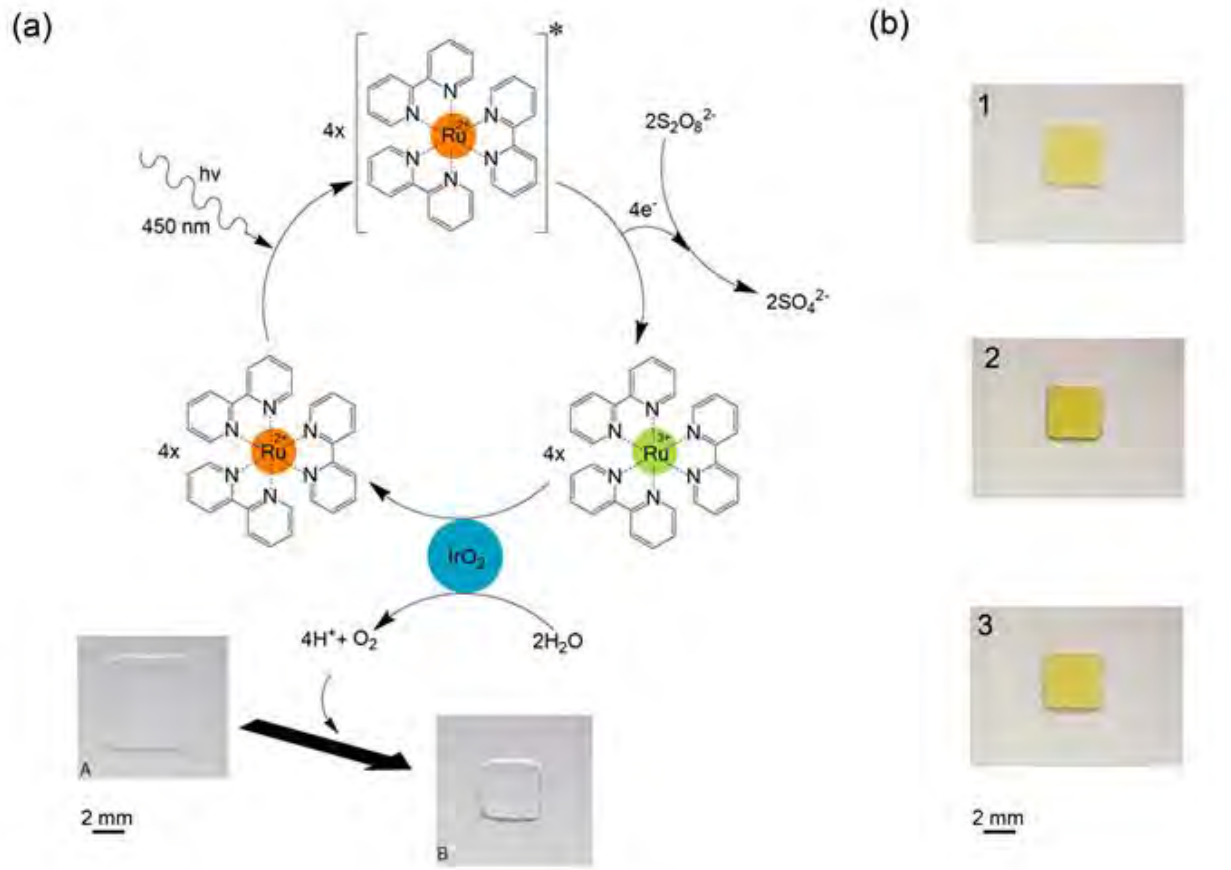

Figure 2: (a)Schematic illustration of the chemistry of the water-splitting reaction and the light induced mechanical movements of polyacrylic acid based hydrogel. a-A, Poly acrylic acid (PAA) gel in basic form, pH=9; a-B, PAA gel in acidic form, pH=2. (b) Demonstration of the self-sustained reversible IrO2 nanocomposite incorporated Ru-PAA polymer performance in air saturated water solution (pH=5.6): b-1, Ru-PAA gel reaches equilibrium; b-2, the gel shrinks at the end of the water-splitting reaction (pH=4.5 at 30mins); b-3, the gel swells back to original size after been moved to dark.

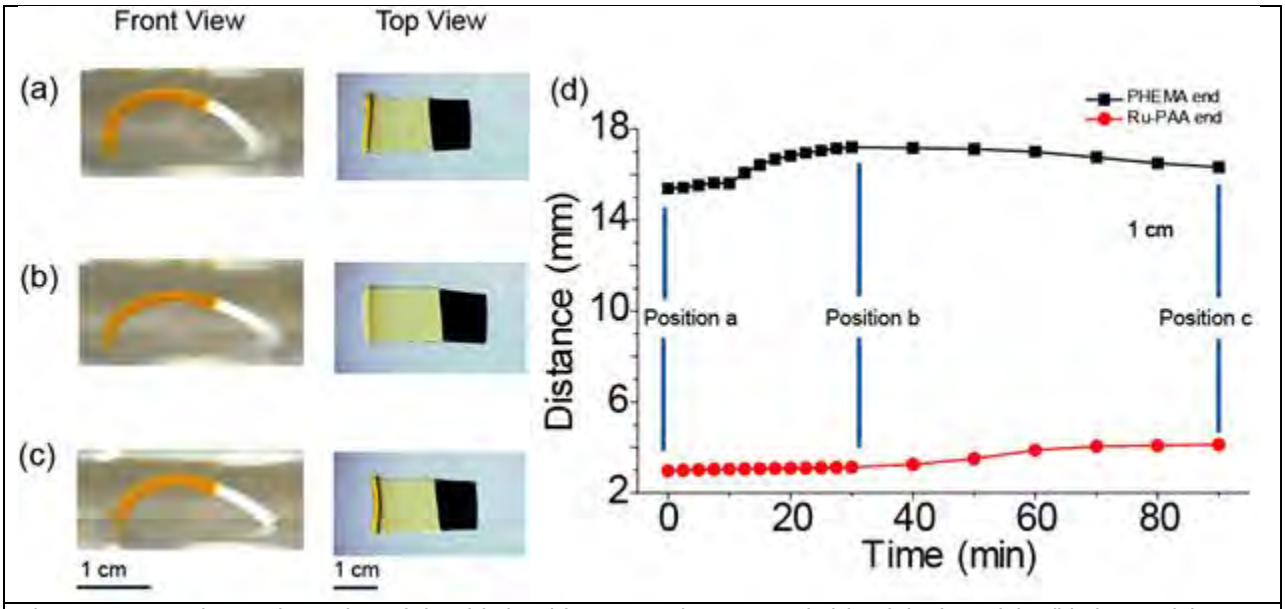

Figure 2: Front view and top view of the side by side Ru-PAA/PHEMA gel: (a) original particle; (b) the particle went through water-splitting reaction; (c) the recovered particle. (d) The distance in between the ends of the particle and the edge of the petri-dish.

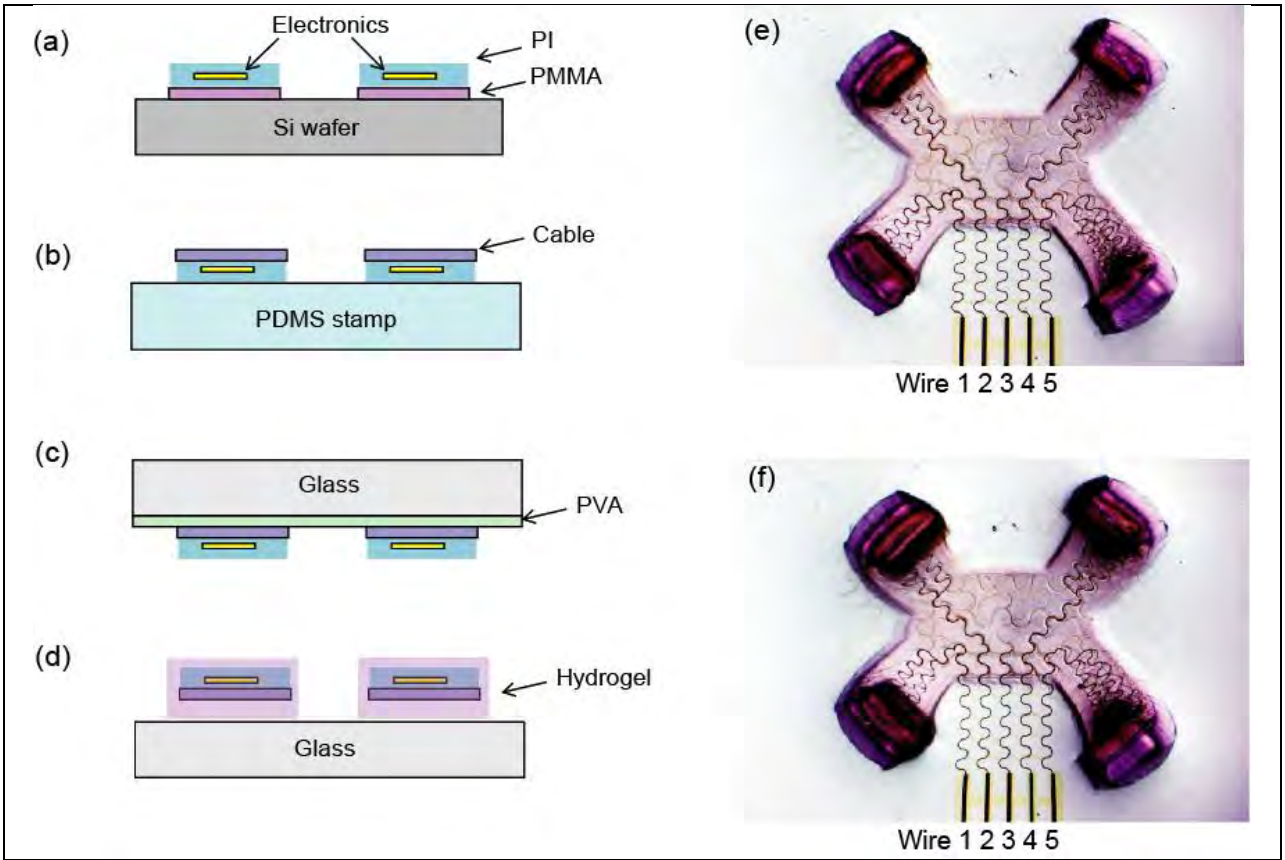

Figure 3: Patterned electronics deposited on silicon wafer; (b) Electronic mesh is trasnfered onto a PDMS stamp and wired with cable; (c) Attach the cabled mesh with PVA/glass; (d) release the mesh into pre-gel solution. (e) and (f) are the before and after of the actual gel was applied to the electrochemical reaction. Wire 1, 2, 4 and 5 are connected as working electrodes; wire 3 is connected as counter and reference electrode.

REFERENCES:

[[1]] Siegel, R.A.; Firestone, B.A., pH-Dependent Equilibrium Swelling Properties of Hydrophobic Poly-Electrolyte Copolymer Gels. *Macromolecules*, **1988**, 21, 3254-3259

[[1]] Kwon, I.C.; Bae, Y.H.; Kim, S.W., Electrically Erodible Polymer Gel for Controlled Release of Drugs, *Nature*, **1991**, 354, 291-293

[[1]] Kontturi, K.; Mafe, S.; Manzanares, J.A.; Svarfvar, B.L.; Viinikka, P, Modeling of the Salt and pH Effects on the Permeability of Grafted Porous Membranes. *Macromolecules*, **1996**, 29, 5740-5746.

[[1]] Holtz, J.H.; Asher, S.A., Polymerized Colloidal Crystal Hydrogel Films as Intelligent Chemical Sensing Materials, *Nature*, **1997**, 389, 829-832.

[[1]] Miyata, T.; Asami, N.; Uragami, T., A Reversibly Antigen-Responsive Hydrogel, *Nature*, **1991**, 399, 766-769.

[1] Yu, Y.; Nakano, M.; Ikeda, T. Directed Bending of a Polymer Film by Light, *Nature*, **2003**, 425, 145.

[[1]] Hara, M.; Waraksa, C.C.; Lean, J.T.; Lewis, B.A.; Mallouk, T.E., Photocatalytic Water Oxidation in a Buffered Tris (2,2'-bipyridyl)ruthenium Complex-Colloidal IrO_2 System, *J. Phys. Chem. A*, **2000**, 104, 5275-5280.

[[1]] Hara, M.; Lean, J.T.; Mallouk, T.E., Photocatalytic Oxidation of Water by Silica-Supported Tris (4,4'-diakyl-2,2'-bipyridyl)ruthenium Polymetic Sensitizers and Colloidal Iridium Oxide, *Chem. Mater.*, **2001**, 13, 4668-4675.

[1] Harriman, A., Pickering, I.J., Thomas, J.M., Christensen, P.A., Metal-Oxides as Heterogeneous Catalysts for Oxygen Evolution under Photochemical Conditions. *J. Chem.Soc. Faraday Trans. 1*. **1988**,84, 2795-2806.

[1] Hoertz, P.G., Kim, Y.I., Youngblood, W.J., Mallouk, W.J., Bidentate Dicarboxylate Capping Groups and Photosensitizers Contol the Size of IrO2 Nanoparticles Catalysts for Water Oxidation, *J. Phys. Chem. B*, **2007**, 111, 6845-6856.

[1] Harriman, A.; Richoux, M.C.; Christensen, P.A.; Mosseri, S.; Neta, P., Redox Reactions with Colloidal Metal Oxides, *J. Chem. Soc., Faraday Trans. 1*. **1987**. 83. 3001-3014

[[1]] Philippova, O.E.; Hourdet, D.; Audebert, R.; Khokhlov, A., pH-Responsive Gels of Hydrophobically Modified Poly(acrylic acid), *Macromolecules*, **1997**, 30, 8278-8285.

[[1]] Eichenbaum, G.M.; Kiser, P.F.; Simon, S.A.; Needham, D., pH and Ion Triggered Volume Response of Anionic Hydrogel Microspheres, *Macromolecules*, **1998**, 31, 5084-5093.

[1] Mack, N.H., Wackerly, J.W., Malyarchuk, V., Rogers, J.A., Moore J.S., Nuzzo, R.G. Oprical Transduction of Chemical Forces, *Nano Letter*, **2007**, 7, 733-737.

[1] Mitrovski, S. M.; Nuzzo, R.G. An Electrochemical Driven Poly(Dimenthylsiloxane) Microfluidic Actuator: Oxygen Sensing and Programmable Flows and pH Gradients. Lab Chip, **2005**, 5, 634-645.

3. NORTHWESTERN UNIVERSITY (GRZYBOWSKI GROUP)

1. Programmable Self-Assembling Systems: Directed assembly of colloids into crystals.

Assembly of colloidal building blocks into complicated structures is of fundamental and technological importance for their applications in photonics[1] and devices[2]. External fields are also frequently used for directing colloids not only for studying the equilibrium behavior[3] but also for drug delivery[4] and cancer therapy[5]. Here we employ precisely controlled, to a micrometer scale, external magnetic fields to direct assembly of nonmagnetic and magnetic colloidal systems into colloidal crystals or core-shell assemblies. It is known that non-magnetic particles dispersed in a ferrofluid can be directed by magnetic field gradients since the pioneering work of Skjeltrop[6]. There is few reports since the work of Skjeltorp, we use nonmagnetic and magnetic particles or a mixture of both in a ferrofluid made from an aqueous solution of holmiumnitrate (which has no durability issues) to control the assembly of these colloids on an alternating magnetic field surface.

We used colloidal particles with different sizes, dispersed in refractive index matching DMSO-water or glycerol-water mixtures. Refractive index matching of the particles was necessary for the imaging purposes but more for the stability of charge-stabilized particles due to the added holmium salt, which decreases the screening length and causes particle aggregation. Refractive index matching enabled us to increase the salt concentration up to 1M without any aggregation of particles. Holmium nitrate concentration was kept between 0.2M-0.4M. This causes an optimum magnetophoretic force for micron-sized spheres.

Colloids dispersed in holmium nitrate solution were let to sediment on top of a nickel grid or pattern, which was placed on top of a magnet as depicted in Figure 1a. Nickel is a ferromagnetic metal and is polarized upon exposure to external magnetic field. When a nickel grid is placed on top of a magnet the metal bars will be polarized and it will form a magnetic grid above the nickel grid. The magnetic field flux over a nickel grid is shown in Fig 1h. As shown also in Fig 1i, numerical calculations of the magnetic field on a nickel grid, the magnetic field fluctuates along the grid holes and bars of the grid. When non-magnetic colloids, dispersed in a paramagnetic fluid, are exposed to such magnetic field pattern, particles will prefer to go towards the low field, as the paramagnetic fluid would be attracted towards the higher fields. The magnetophoretic drive of the colloids to the lower field was observed for 1.2 μm particles on a grid with 7μm holes, seen in Fig 1b. We also managed to do this assembly on a single particle level by sedimenting 50 μm particles on square and hexagonal grids with 43 μm holes, seen in Fig. 1e and Fig. 1g, respectively. Fig 1c, 1d and 1f show other types of assembly where 1.2 μm particles assemble on 1.4μm wells in 1c, on 3 μm wells in 1d and on 5-fold quasicrystalline 2 μm wells in 1f.

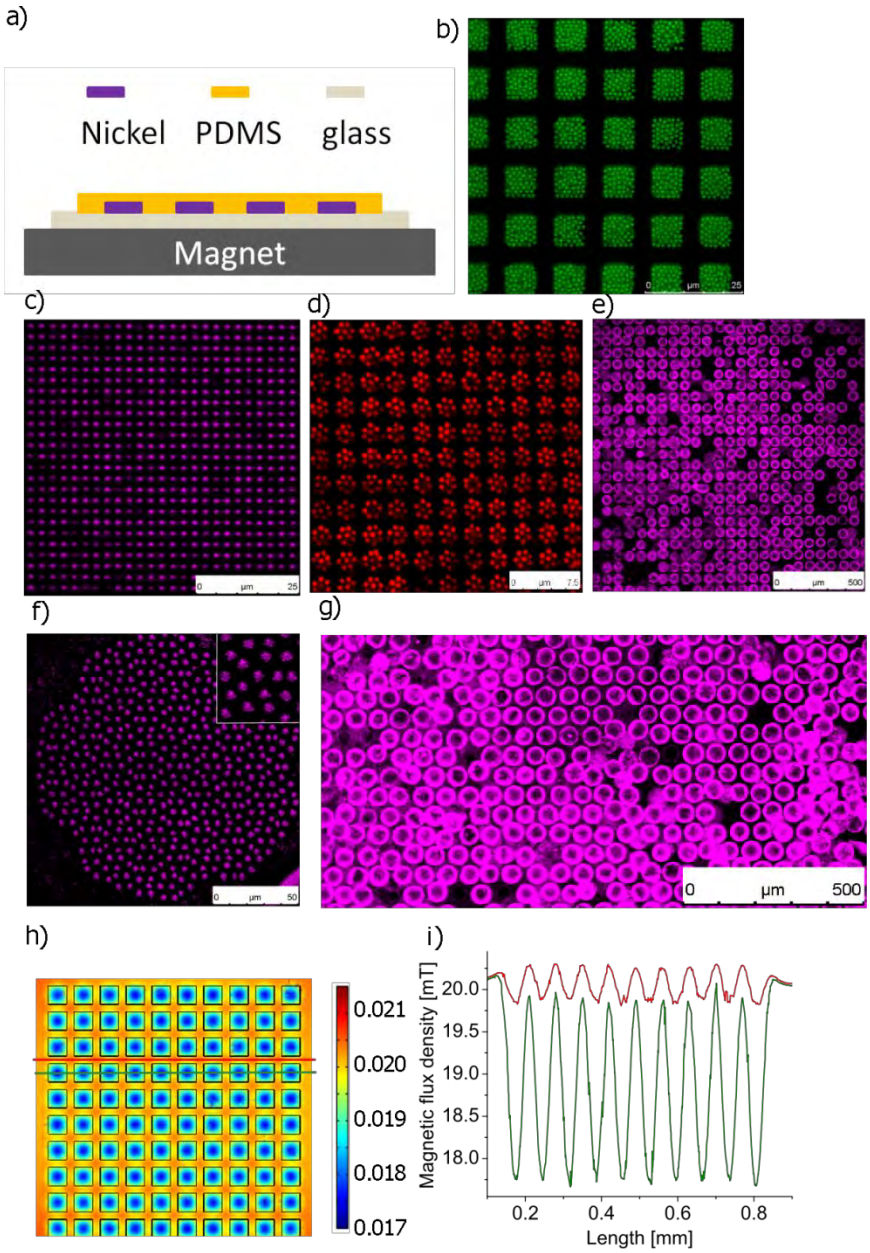

Fig 1. **(a)** Side view of the sample cell construction. Single type of colloids directed towards the holes of different types of TEM grids, **(b)** 1.2 μm colloids assembled on the holes of a TEM grid with a 7 μm hole size, **(c)** 1.2 μm colloids assembled on the holes of a lithographically made nickel grid with holes of 1.4 μm, **(c)** 1.2 μm colloids assembled on the holes of a TEM grid with a 7 μm hole size, **(d)** 800 nm silica particles assembled in 3.0 μm sized magnetic wells, where only 7 particles fit into the well, **(e)** 50 μm colloids assembled on the holes of a square TEM grid with 43 μm hole size, **(f)** 1.2 μm colloids assembled on 5-fold quasicrystalline ordered wells, **(g)** 50 μm colloids assembled on the holes of a hexagonal TEM grid with 43 μm hole size, **(h)** Numerical calculation of the magnetic flux density over a Nickel grid, placed on top of a magnet, **(i)** The magnetic flux density on the lines (red and green) depicted at (h) along the holes of the grid (green) and along the intersections of the grid (red).

When a mixture of non-magnetic colloids with different sizes was sedimented on nickel grids, we observed segregation of these particles in a core-shell manner. Magnetophoretic forces depend on the volume of the spheres and for a larger sphere the force is larger to the r^3, where r is the radius of the colloid. This difference in the applying forces plays the role to push the larger 1.2 μm particles to the holes first and the smaller 800 nm ones afterwards, which causes the formation of the core-shell construction seen in Fig 2a-c. Fig 2a shows the confocal microscopy image of the 800 nm and Fig 2a shows the image of the 1.2 μm particles that form the core of the assembly. Fig2c is an overlay of the images given in Fig 2a and Fig 2b that clearly shows the core shell structure. Fig 2d is a constructed image from the same z-stack of the images shown in Fig2a-c and it shows the side view of the particles in z-axis. We made the same experiment with 5 μm and 1.2 μm particles` mixture on a grid with 7 μm holes and the result was formation of raspberry like structures due to the size segregation, as shown in Fig. 2e.

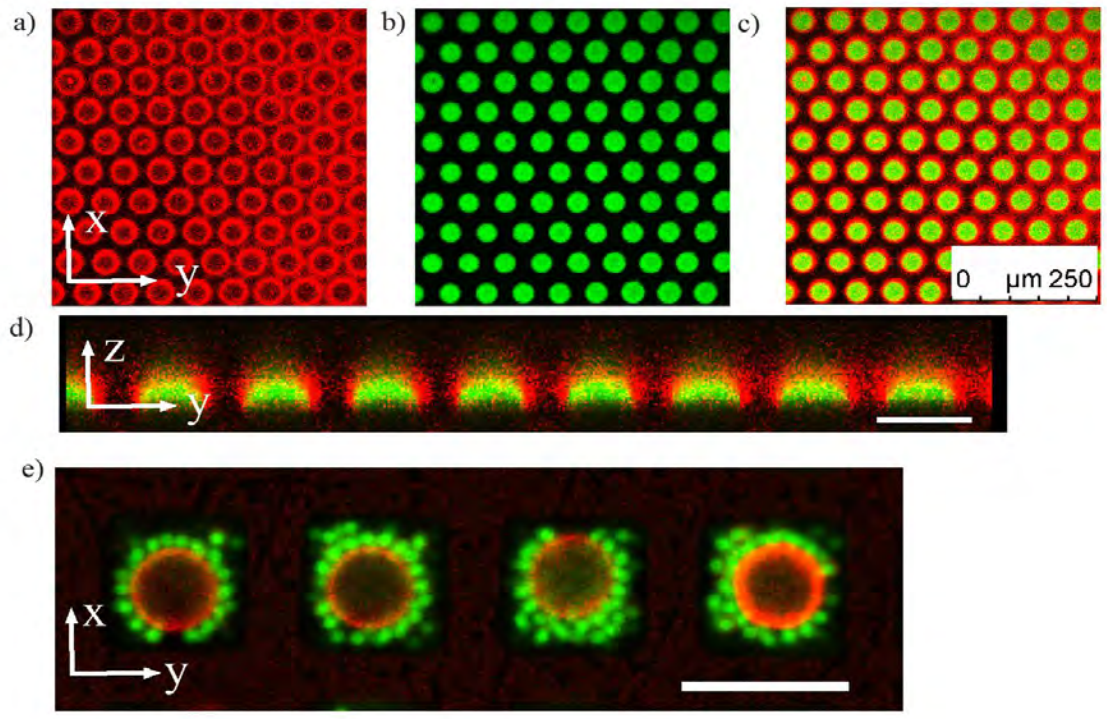

Fig 2. Binary mixtures of colloidal particles driven towards the low magnetic field regions with a phase separation due to size difference, **(a)** fluorescence image of RITC labeled 800 nm silica particles, which form a shell around the 1.2 μm FITC labeled silica colloids shown in (b). **(b)** Fluorescence image of FITC labeled particles with a size of 1.2 μm, these particles are driven to the core of the assembly due to their larger size. **(c)** Overlay of the images shown in (a) and (b), which shows clearly the core-shell structure, **(d)** side view of the z-stack along a line shown in (c) (Scale bar 40 μm). **(e)** Raspberry-like assembly of 5 μm silica particles labeled with RITC, which are surrounded by 1.2 μm FITC labeled particles (Scale bar 10 μm).

With the fact of an underlying magnetic grid it is expected that a mixture of magnetic and non-magnetic particles will phase separate. When we sedimented a mixture of magnetic and non-magnetic particles of about 1μm size on a grid with 43 μm holes, particles phase separated on the grid bars and the holes. Magnetic particles were driven towards the grid bars with a higher concentration on the crosses of the bars, whereas the non-magnetic particles filled the holes of the grids, as seen in Fig. 3a. It should be noted that the magnetic field is stronger on the crossings of the bars as can also be seen in Fig. 1f and this causes the magnetic particles to concentrate more on these spots.

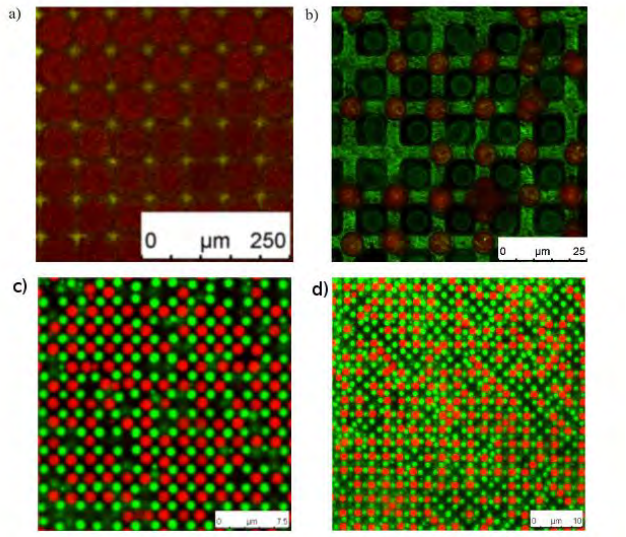

Fig 3. Confocal microscopy images of binary mixtures of colloids with different magnetization (magnetic susceptibility), **(a)** non-magnetic 900nm silica particles labeled with RITC (red) and 800 nm magnetic silica particles labeled with FITC (green), that are phase separated on a nickel grid with 43 μm holes, **(b)** non-magnetic particles of 5μm size labeled with FITC(green), and 5.8 μm magnetic particles labeled with Alexa Fluor 660 (red), **(c)** and **(d)** 1μm sized non-magnetic (green), and magnetic (red) particles on 1.4 μm pitch sized grids.

Magnetic and non-magnetic particles with 5 μm and 5.8 μm sizes, respectively, formed a 2D binary crystal when sedimented on a grid with 7 μm holes and 12 μm pitch size. Here again the magnetic particles mostly preferred the intersection of the bars which enabled the formation of the binary square lattice shown in Fig. 3b. Fig. 3c and 3d shows 1 μm sized non-magnetic (green), and magnetic (red) particles on 1.4 μm pitch sized grids, these particles assemble into AB crystals in Fig 3c whereas they form an AB_2 type crystal in Fig 3d. Formation of these ordered assemblies are highly coordinated with the underlying nickel grid which gives the opportunity to design diverse structures.

We also investigated the behavior of magnetic and non-magnetic particle mixtures with different sizes. We used 1.2 μm non-magnetic silica particles and 5.8 μm magnetic particles. In a uniform magnetic field these particles were oppositely polarized due to the magnetic susceptibility difference between the

particles and the solvent[7]. For nonmagnetic particles and magnetic particles dispersed in a paramagnetic fluid the induced dipoles are in opposite directions and this causes an attraction between the particles. Here due to the size ratio smaller particles cover the big one and form raspberry like structures, shown in Fig 4a. These raspberries were similar to the ones shown in Fig 2e, but the underlying physics was totally different. However, this inverse-dipolar attraction between the magnetic and non-magnetic particles was overcome when particles were on a gradient of magnetic field as on a grid shown in Fig 4b. The grid with the 7 μm hole sizes broke the attraction between the particles and directed the non- magnetic particles to the holes and the magnetic particles to the grid bars. Interplay of the two different phenomena could be used in a ternary system to make raspberry structures both in a gradient and in homogenous field. Ternary system composed of magnetic 5.8 μm particles and non-magnetic 5 μm and 1.2 μm particles. In a homogenous field magnetic 5.8 μm particles and non-magnetic 1.2 μm particles form raspberry particles where 5μm non-magnetic particles were mostly left out of the attraction shell. When the ternary particle system was brought on the grid the magnetic particles were driven on the grid bars and the nonmagnetic large and small particles formed raspberry structures in the grid holes, both raspberry structures in homogeneous and alternating field strengths were shown in Fig 4c and d, respectively.

In summary, we have shown different assemblies of nonmagnetic and magnetic particles at different length scales between 1-50 μm by using magnetic field gradients for directing both magnetic and non-magnetic particles. We would like to point out that our results could be of high interest for potential applications in optical devices or in delivery systems.

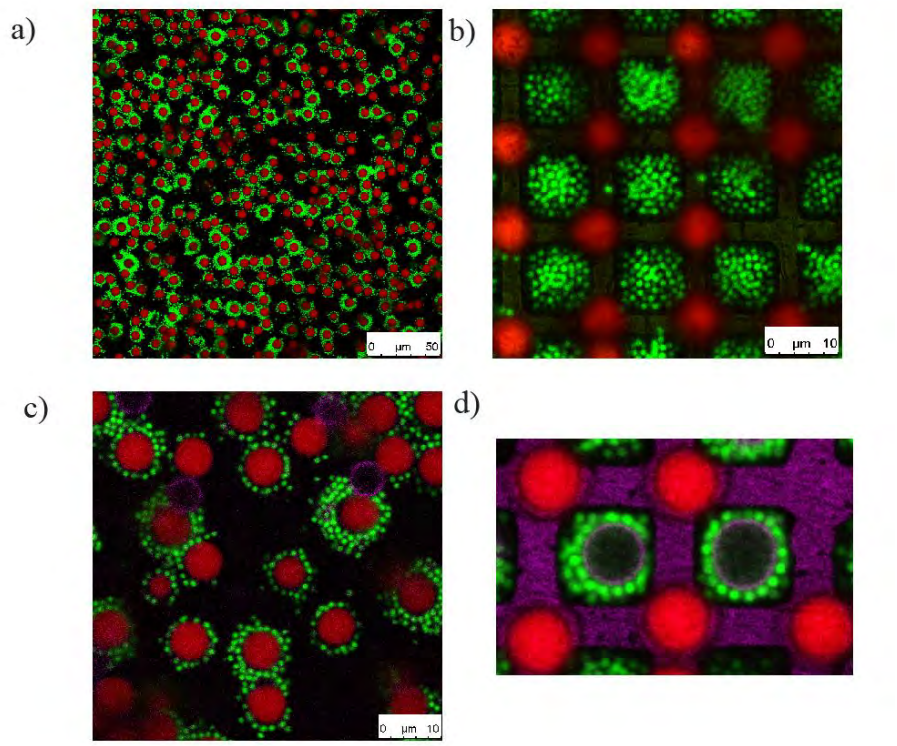

Fig 4. Confocal microscopy images of binary mixtures of binary (a,b) and ternary (c,d) colloids with different magnetization (magnetic susceptibility) and different size, **(a)** non-magnetic 1.2µm silica particles labeled with FITC (green) and 5.8µm magnetic particles labeled with Alexa Fluor 660 (red), that are in an homogenous magnetic field, **(b)** same particle system separated on a nickel grid with 7µm hole sizes, **(c)** non-magnetic particles of 5µm size labeled with RITC (purple), 5.8µm magnetic particles labeled with Alexa Fluor 660 (red) and non-magnetic 1.2µm FITC labeled particles (green) in a homogenous magnetic field, **(d)** same particles system as in (c) separated on a nickel grid with 7 µm hole sizes.

REFERENCES:

1. Xia, Y., Gates, B. & Li, Z.-Y. Self-Assembly Approaches to Three-Dimensional Photonic Crystals. *Adv. Mater.* **13**, 409-413 (2001).

2. Elghanian, R., Storhoff, J.J., Mucic, R.C., Letsinger, R.L. & Mirkin, C.A. Selective Colorimetric Detection of Polynucleotides Based on the Distance-Dependent Optical Properties of Gold Nanoparticles. *Science* **277**, 1078 -1081 (1997).

3. Yethiraj, A., Thijssen, J.H.J., Wouterse, A. & van Blaaderen, A. Large Area Electric Field Induced Colloidal Single Crystals for Photonic Applications. *Advanced Materials* **16**, 596-600 (2004).

4. Son, S.J., Reichel, J., He, B., Schuchman, M. & Lee, S.B. Magnetic Nanotubes for Magnetic-Field-Assisted Bioseparation, Biointeraction, and Drug Delivery. *Journal of the American Chemical Society* **127**, 7316-7317 (2005).

5. Hergt, R., Dutz, S., Müller, R. & Zeisberger, M. Magnetic particle hyperthermia: nanoparticle magnetism and materials development for cancer therapy. *J. Phys.: Condens. Matter* **18**, S2919-S2934 (2006).

6. Skjeltorp, A.T. One- and Two-Dimensional Crystallization of Magnetic Holes. *Phys. Rev. Lett.* **51**, 2306 (1983).

7. Erb, R.M., Son, H.S., Samanta, B., Rotello, V.M. & Yellen, B.B. Magnetic assembly of colloidal superstructures with multipole symmetry. *Nature* **457**, 999-1002 (2009).

8. Yellen, B.B. & Friedman, G. Programmable Assembly of Colloidal Particles Using Magnetic Microwell Templates. *Langmuir* **20**, 2553-2559 (2004).